ACS APPLIED MATERIALS & INTERFACES

Research Article

www.acsami.org

Ruthenium Sensitizers with a Hexylthiophene-Modified Terpyridine Ligand for Dye-Sensitized Solar Cells: Synthesis, Photo- and Electrochemical Properties, and Adsorption Behavior to the TiO_2 Surface

Hironobu Ozawa, Yasuyuki Yamamoto, Hiroki Kawaguchi, Ryosuke Shimizu, and Hironori Arakawa*

Department of Industrial Chemistry, Faculty of Engineering, Tokyo University of Science, 12-1, Ichigaya-Funagawara, Shinjuku, Tokyo, 162-0826, Japan

ABSTRACT: Two novel ruthenium sensitizers with a hexylthiophene-modified terpyridine ligand (**TUS-35** and **TUS-36**) were synthesized to improve the molar absorptivity of the previously reported ruthenium sensitizer (TBA)[Ru{4′-(3,4-dicarboxyphenyl)-4,4″-dicarboxyterpyridine}$(NCS)_3$], TBA = tetrabutylammonium (**TUS-21**). A relatively strong absorption appeared at ∼380 nm, and the molar absorption coefficient at the metal-to-ligand charge transfer (MLCT) band decreased in **TUS-35** by introducing a 2-hexylthiophene unit to the 5-position of the terpyridine-derived ligand. For comparison, a relatively strong absorption was observed at ∼350 nm without decreasing the molar absorption coefficient at the MLCT band in **TUS-36** by introducing a 2-hexylthiophene unit to the 4-position of the terpyridine-derived ligand. On the other hand, the energy levels of the highest occupied molecular orbitals and the lowest unoccupied molecular orbitals of these two sensitizers were found to be almost equal to those of **TUS-21**. The adsorption behavior of **TUS-35** and **TUS-36** was similar to that of (TBA)[Ru{4′-(3,4-dicarboxyphenyl)terpyridine}$(NCS)_3$] (**TUS-20**), which binds to the TiO_2 surface by using the 3,4-dicarboxyphenly unit, rather than that of **TUS-21**, which adsorbs to the TiO_2 photoelectrode using one of the carboxyl groups at the terminal pyridines of the terpyridine-derived ligand. Therefore, **TUS-35** and **TUS-36** are considered to bind to the TiO_2 surface by using the 3,4-dicarboxyphenly unit just like **TUS-20**. The dye-sensitized solar cells (DSCs) with **TUS-35** and **TUS-36** showed a relatively lower conversion efficiency (6.4% and 5.7%, respectively) compared to the DSC with **TUS-21** (10.2%). Open-circuit photovoltage decay and electrochemical impedance spectroscopy measurements revealed that the promoted charge recombination and/or charge transfer of the injected electrons in the TiO_2 photoelectrode is a main reason for the inferior performances of **TUS-35** and **TUS-36**.

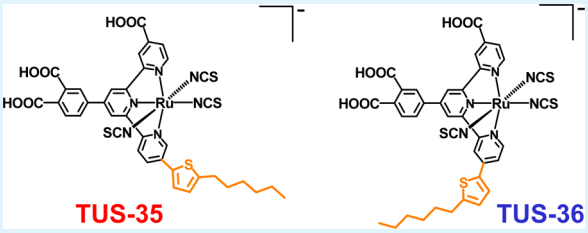

KEYWORDS: *dye-sensitized solar cell, ruthenium sensitizer, terpyridine, thiophene, adsorption behavior*

INTRODUCTION

In the last two decades, continuous efforts have been devoted to increase the light-to-electrical energy conversion efficiency of dye-sensitized solar cells (DSCs) since the pioneering studies were reported in the early 1990s.[1−5] A large number of molecular sensitizers, such as ruthenium-complex sensitizers[6−16] and zinc porphyrin sensitizers,[17−21] has been synthesized for the improvement of conversion efficiency of DSCs because the solar cell performances of the DSCs depend strongly on the photosensitizing ability of these sensitizers. One of the most important requirements for the highly efficient sensitizers is a wide absorption, which covers whole visible and near-IR region as high as nearly 1000 nm, with a large molar absorptivity. In addition, suitable energy levels of highest occupied molecular orbital (HOMO) and lowest unoccupied molecular orbitals (LUMO) are also important requirements for the highly efficient sensitizers because these enable effective electron-transfer reactions in the DSCs such as an electron injection from the photoexcited sensitizers into the conduction band of TiO_2 and a regeneration of the resulting oxidized sensitizers by the redox mediator in the electrolyte solution. $(TBA)_3$[Ru(Htcterpy)$(NCS)_3$] (Black dye; TBA = tetrabutylammonium; tcterpy = 4,4′,4″-tricarboxy-2,2′:6′,2″-terpyridine; see Figure 1) is well-known to be a highly efficient ruthenium sensitizer that satisfies the above requirements, and the conversion efficiency above 11.0% has been achieved in the Black-dye-based DSCs.[7,22−29] Various kinds of structural modifications of Black dye have been thus far carried out to synthesize novel highly efficient ruthenium sensitizers that exhibit the superior conversion efficiency compared to Black dye.[30−38] Among these attempts, introduction of a chromophore unit to the terpyridine-derived ligand is considered to be one of the effective methods to enhance the performance of Black dye because the molar absorptivity of Black dye at the whole visible region is smaller than that of the other famous and efficient ruthenium sensitizers such as N719 and C101.

Received: October 26, 2014
Accepted: January 14, 2015
Published: January 14, 2015

DOI: 10.1021/am507442s
ACS Appl. Mater. Interfaces 2015, 7, 3152−3161

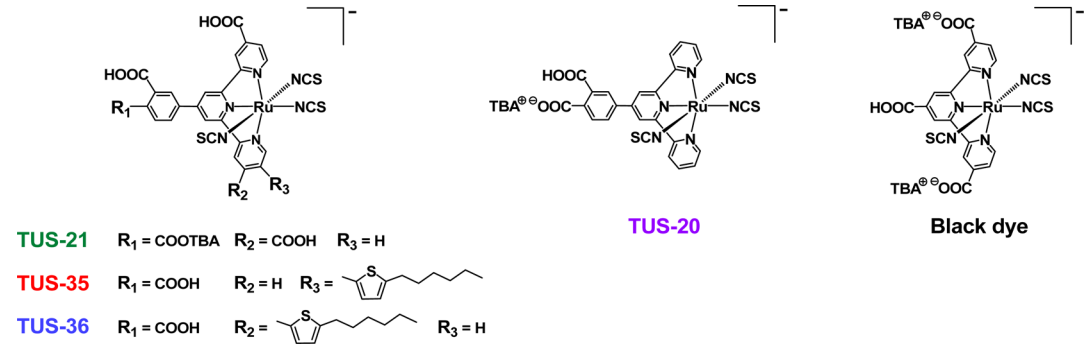

Figure 1. Molecular structures of **TUS-20**, **TUS-21**, **TUS-35**, **TUS-36**, and Black dye.

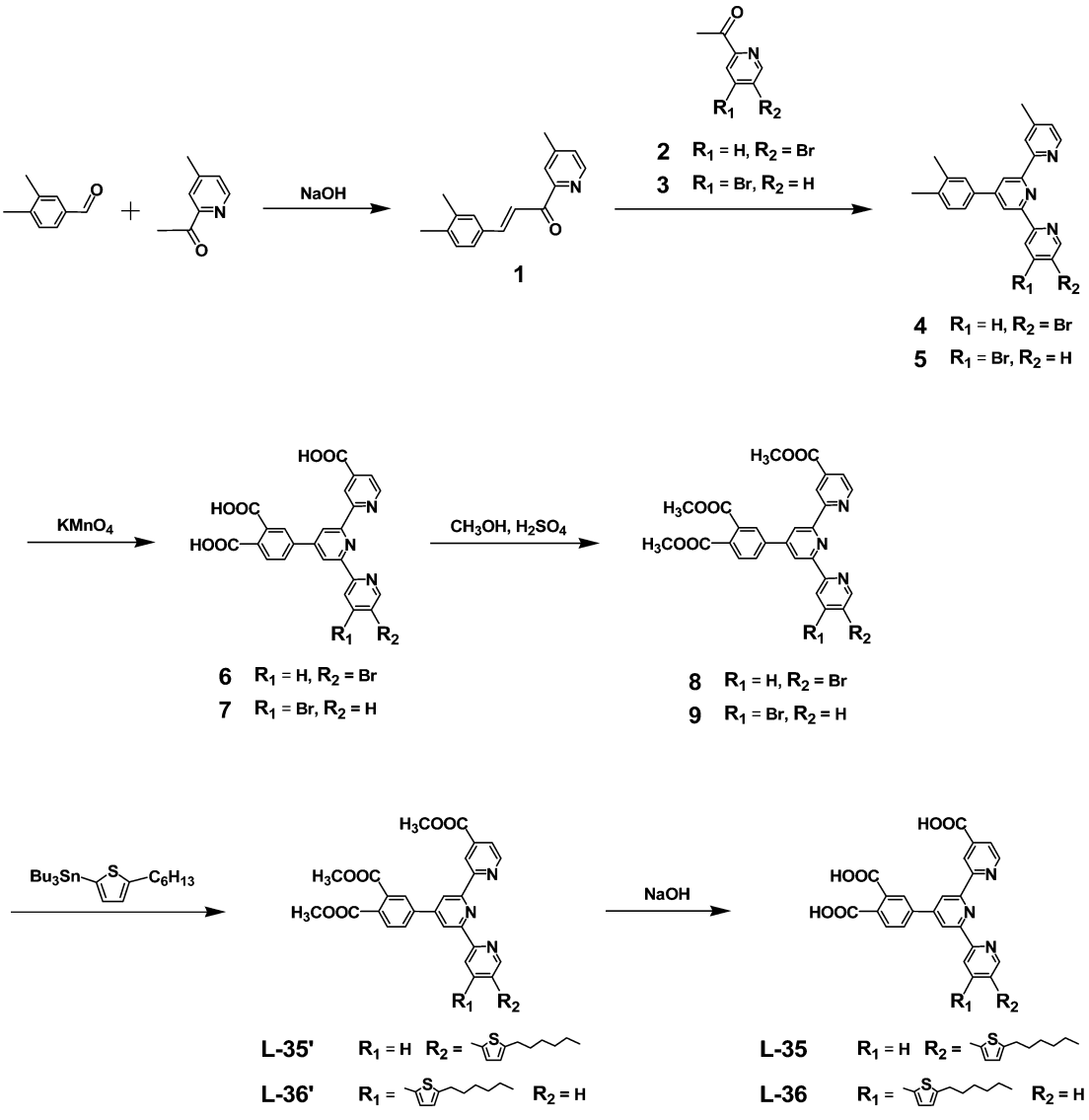

Figure 2. Synthetic scheme of the hexylthiophene-modified terpyridine-derived ligands (**L-35** and **L-36**).

In this context, continuous studies on the development of highly efficient ruthenium sensitizers with a tcterpy-derived ligand have been also carried out in our group.[39−43] Recently, we reported that (TBA)[Ru{4′-(3,4-dicarboxyphenyl)-4,4″-dicarboxyterpyridine}(NCS)$_3$] (**TUS-21**, Figure 1), which is a structural analogue of Black dye, has a broad absorption until ∼850 nm with a molar absorptivity larger than that of Black dye, even though **TUS-21** does not possess a chromophore unit.[42] The DSC with **TUS-21** showed relatively higher conversion efficiency under AM 1.5 irradiation (10.2%), although it is slightly lower compared to that of the DSC with Black dye (10.8%).[42] In the study, the obtained photocurrent density (Jsc) value in the DSC with **TUS-21** (21.1 mA/cm^2) was found to be slightly smaller than that obtained in the DSC with Black dye (21.6 mA/cm^2), and hence the obtained conversion efficiency in the DSC with **TUS-21**

DOI: 10.1021/am507442s
ACS Appl. Mater. Interfaces 2015, 7, 3152−3161

was slightly lower compared to that of the DSC with Black dye. Therefore, further structural modifications of **TUS-21**, which aim to increase the molar absorptivity, are expected to enhance the conversion efficiency of the DSC with **TUS-21**.

On the other hand, we have also reported that introduction of a chromophore unit, such as a 2-hexylthiophene unit, to the terpyridine-derived ligands of ruthenium sensitizers is an effective method for increasing the molar absorptivity of ruthenium sensitizers at ~400 nm and for improving effectively incident photon-to-current conversion efficiency (IPCE) of the DSCs at this wavelength range.[40,43] In this study, two novel ruthenium sensitizers with a hexylthiophene-modified terpyridine-derived ligand (**TUS-35** and **TUS-36**, Figure 1) were synthesized to be improved models of **TUS-21**. Since one of the COOH groups at the terminal pyridines of the terpyridine-derived ligand of **TUS-21** does not participate in the adsorption to the TiO_2 photoelectrode,[42] the 2-hexylthiophene unit was introduced to the 4- or 5-position of the terminal pyridine of terpyridine-derived ligand to improve the molar absorptivity. Here we report synthesis, photo- and electrochemical properties, and the solar cell performances of the DSCs with these two sensitizers. In addition, effects of the position of the chromophore unit at the terpyridine-derived ligand on the photo- and electrochemical properties and on the performances of the DSCs will also be reported.

RESULTS AND DISCUSSION

Synthesis. The synthetic route of novel hexylthiophene-modified terpyridine-derived ligands (**L-35** and **L-36**) is shown in Figure 2. The key intermediates (5- or 4-bromo-substituted terpyridine derivative; **6** and **7**, respectively) were synthesized by the reaction of **1** and 2-acetyl-5-bromopyridine[44] (or 2-acetyl-4-bromopyridine[43]), followed by the oxidation of three methyl groups of **4** and **5** by $KMnO_4$. Since the solubility of **6** and **7** is very low in common organic solvents; esterification of three COOH groups of **6** and **7** was carried out prior to the cross-coupling reaction. Cross-coupling reaction of **6** (or **7**) and tributyl(5-hexylthiophene-2-yl)stannane[45,46] in the presence of $Pd(PPh_3)_4$ afforded **L-35′** (or **L-36′**) in 50−60% yield. Finally, deprotection of methyl esters of **L-35′** (or **L-36′**) was carried out in advance because decomposition of ruthenium-complex sensitizers might occur under the strong basic condition. The total synthetic yield over six steps was below 10%. **TUS-35** and **TUS-36** were synthesized by the reaction of **L-35** (or **L-36**) and $RuCl_3 \cdot 3H_2O$, followed by the reaction of KSCN. Multiple purifications of the crude product were carried out by a silica gel column chromatography. These two novel sensitizers were characterized successfully by ^1H NMR spectroscopy, electrospray ionization time-of-flight mass spectrometry (ESI-TOF MS), and elemental analysis. The amounts of TBA^+ contained in **TUS-35** and **TUS-36** were estimated to be 1.25 from ^1H NMR spectra and elemental analysis. A single molecule of TBA^+ exists as a countercation of each sensitizer; therefore, one of the H^+ of three COOH groups of each sensitizer is replaced partially by TBA^+. In the case of **TUS-21**, the amount of TBA^+ was reported to be 2.0, and the H^+ of the COOH group at the 4-position of the phenyl unit was reported to be replaced perfectly by TBA^+.[42] From the ^1H NMR spectra, the H^+ of the COOH group at the 4-position of the phenyl unit in each novel sensitizer is also considered to be replaced partially by TBA^+.

Photo- and Electrochemical Studies. Absorption spectra of **TUS-21**, **TUS-35**, **TUS-36**, and Black dye in dimethylformamide (DMF) are shown in Figure 3. As reported previously,

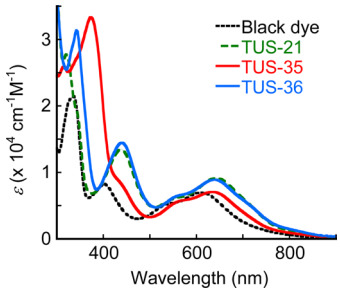

Figure 3. Absorption spectra of **TUS-21**, **TUS-35**, **TUS-36**, and Black dye in DMF.

TUS-21 has the molar absorption coefficient larger than that of Black dye in the whole visible region, presumably due to the introduction of the 3,4-dicarboxyphenyl unit at the 4′-position of the terpyridine ligand.[42] In the case of **TUS-35**, a relatively strong absorption at ~380 nm, which is assignable to the intraligand $\pi-\pi^*$ transition from the thiophene moiety to the terpyridine one,[32,33] appeared, and the molar absorption coefficient at the wavelength range beyond 410 nm was decreased by introducing a hexylthiophene unit at the 5-position of the terpyridine-derived ligand instead of the COOH group at the 4-position. As reported recently, loss of the COOH group at the 4-position of the terpyridine ligand induces the reduction of the transition dipole of the metal-to-ligand charge transfer (MLCT) transition, which results in the decrement of the molar absorption coefficient at the MLCT band of the ruthenium complexes with a 4,4′,4″-tricarboxyterpyridine-derived ligand.[40,43] Therefore, the observed decrement in the molar absorption coefficient at the MLCT band of **TUS-35** seems to be attributed to this reason. For comparison, in the case of **TUS-36**, a relatively strong absorption at ~350 nm appeared without decreasing the molar absorptivity at the wavelength range beyond 400 nm by replacing the COOH group at the 4-position of the terpyridine-derived ligand into the hexylthiophene unit. This result suggests that decrease of the molar absorption coefficient at the MLCT band of the ruthenium complexes with a 4,4′,4″-tricarboxyterpyridine-derived ligand could be prevented by introducing a suitable substituent instead of the COOH group at the 4-position of the terpyridine-derived ligand. In addition, these results indicate clearly that the position of the chromophore unit at the terpyridine-derived ligand affects largely the photochemical properties of ruthenium sensitizers with a terpyridine-derived ligand. Therefore, the position of the chromophore unit at the terpyridine-derived ligand seems to also affect largely the solar cell performances of the DSCs.

Electrochemical measurements were conducted to determine the energy levels of HOMOs of **TUS-35** and **TUS-36**. Quasi-reversible oxidation waves corresponding to the $Ru^{II/III}$ oxidations were observed at 0.62 and 0.59 V versus SCE in the DMF solutions of **TUS-35** and **TUS-36**, respectively (Table 1). These values were only slightly higher than those of **TUS-21** and Black dye; therefore, regeneration of the oxidized **TUS-35** and **TUS-36** by I^- seems to occur effectively in the DSCs with these sensitizers. On the other hand, the estimated energy levels of LUMOs of **TUS-35** and **TUS-36** were very close to those of **TUS-21** and Black dye, suggesting that electron injection from the photoexcited **TUS-35** and **TUS-36** into the conduction band of TiO_2 is thermodynamically possible. These results indicate clearly that the position of the

DOI: 10.1021/am507442s
ACS Appl. Mater. Interfaces 2015, 7, 3152−3161

Table 1. Electrochemical Properties of TUS-21, TUS-35, TUS-36, and Black Dye[a]

sensitizer	E_{HOMO} [V vs SCE]	E_{0-0}[b] [V]	E_{LUMO} [V vs SCE]
TUS-21[c]	0.68	1.61	−0.93
TUS-35	0.62	1.60	−0.98
TUS-36	0.59	1.56	−0.97
Black dye[c]	0.66	1.61	−0.95

[a]The E_{HOMO} of **TUS-35** and **TUS-36** was measured in DMF solution containing 0.1 M $LiClO_4$. [b]The E_{0-0} was calculated using the onset wavelength of the absorption spectrum. [c]Data taken from ref 42.

chromophore unit at the terpyridine-derived ligand affect only slightly the energy levels of HOMO and LUMO, even though it affects largely the photochemical properties of the ruthenium sensitizers as mentioned above. This finding is quite important information for the development of highly efficient ruthenium sensitizers.

Density Functional Theory Molecular Orbital Calculations. Density functional theory (DFT) molecular orbital (MO) calculations were conducted to investigate the distribution of frontier MOs of **TUS-35** and **TUS-36**. As shown in Figure 4, HOMO and HOMO−1 of these **TUS** sensitizers populated dominantly at the Ru^{II} atom and two axial NCS ligands. LUMO of each **TUS** sensitizer located largely at the terminal 4-carboxypyridine of the terpyridine-derived ligand. LUMO+1 of each **TUS** sensitizer populated mainly at both the central pyridine and the hexylthiophene-modified pyridine of the terpyridine-derived ligand. Important point is that LUMO+2 of each **TUS** sensitizer located largely at the 3,4-dicarboxyphenyl unit. These results suggest that effective electron injection from the photoexcited **TUS-35** or **TUS-36** into the conduction band of TiO_2 occurs if these **TUS** sensitizers adsorb to the TiO_2 photoelectrode using the COOH group at the terminal pyridine of the terpyridine-derived ligand. On the other hand, these results also suggest that effective electron injection does not occur if these **TUS** sensitizers adsorb to the TiO_2 photoelectrode using the 3,4-dicarboxyphenyl unit because the electron transfer from the terpyridine unit to the 3,4-dicarboxyphenyl one is thermodynamically unfavorable, and the path length of this electron injection reaction is relatively longer in this case. It was reported recently that LUMO and LUMO+1 of **TUS-21** located over the terpyridine unit, and LUMO+2 populated mainly at the 3,4-dicarboxyphenyl unit.[42] In addition, it was also reported that **TUS-21** adsorbed to the TiO_2 photoelectrode using one of the COOH groups at the terminal pyridines of the terpyridine-derived ligand as shown in Figure 6.[42] Therefore, effective electron injection occurs, and hence the conversion efficiency above 10% was obtained in the DSC with **TUS-21**.[42] A conversion efficiency higher than 10% is also expected in the DSCs with **TUS-36** if this sensitizer adsorbs to the TiO_2 photoelectrode using the COOH group at the terminal pyridine of the terpyridine-derived ligand just like **TUS-21**. However, a relatively lower conversion efficiency might be obtained in the case that **TUS-36** adsorbs to the TiO_2 photoelectrode using the 3,4-dicarboxyphenyl unit.

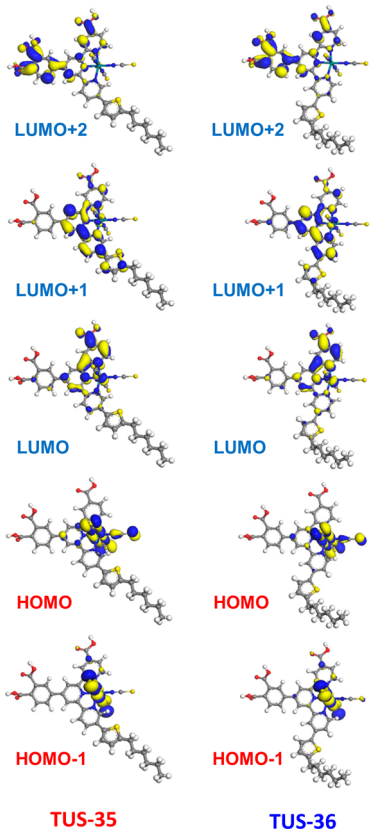

Figure 4. Frontier molecular orbitals of **TUS-35** and **TUS-36** in acetonitrile.

Adsorption Behavior of Dyes. Adsorption behavior of **TUS-35** and **TUS-36** to the TiO_2 surface was investigated to obtain insight into the adsorption manners of these **TUS** sensitizers because adsorption manners of these **TUS** sensitizers at the TiO_2 surface are considered to affect largely the electron injection process and the conversion efficiency of the DSCs as mentioned above. As reported previously, (TBA)[Ru{4′-(3,4-dicarboxyphenyl)terpyridine}$(NCS)_3$] (**TUS-20**, Figure 1) has a superior adsorption to the TiO_2 surface due to the presence of the 3,4-dicarboxyphenyl unit as an anchor group.[39,41] For example, the adsorption rate of **TUS-20** is faster than that of Black dye, and the maximum amount of **TUS-20**-adsorption is larger than that of Black dye.[39,41] Moreover, some amount of adsorbed **TUS-20** could not be desorbed from the TiO_2 photoelectrode by immersing in a NaOH solution for 1 d, while all the adsorbed Black dye could be desorbed perfectly within a few minutes by the same treatment.[39,41] That is to say, these results suggest that ruthenium sensitizers showing such a superior adsorption property adsorb to the TiO_2 photoelectrode using a 3,4-dicarboxyphenyl unit. Among zinc porphyrin sensitizers, such a superior adsorption behavior was also observed in the zinc porphyrin sensitizer having a dicarboxyphenyl unit as an anchor group.[47] As shown in Figure 5, **TUS-20** showed actually a superior adsorption property compared to Black dye. On the other hand, the adsorption behavior of **TUS-21** was quite similar to that of Black dye, even though **TUS-21** also possesses the 3,4-dicarboxyphenyl unit. In addition, all the adsorbed **TUS-21** was desorbed from the TiO_2 photoelectrode perfectly within a few minutes just like Black dye. Together with the results of attenuated total reflection IR measurements, it is reported that **TUS-21** adsorbs to the TiO_2 photoelectrode using one of the COOH groups at the terminal pyridines of the terpyridine-derived ligand as shown in Figure 6.[42] In the cases of **TUS-35** and **TUS-36**, the adsorption behaviors were similar to that of **TUS-20** rather than those of **TUS-21** and Black dye.

DOI: 10.1021/am507442s
ACS Appl. Mater. Interfaces 2015, 7, 3152−3161

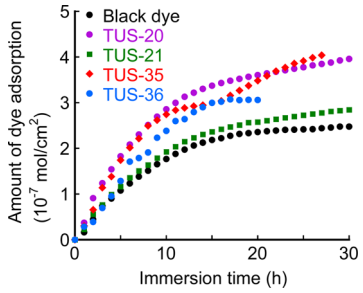

Figure 5. Adsorption isotherms of **TUS-20**, **TUS-21**, **TUS-35**, **TUS-36**, and Black dye to the TiO_2 photoelectrodes at 20 °C.

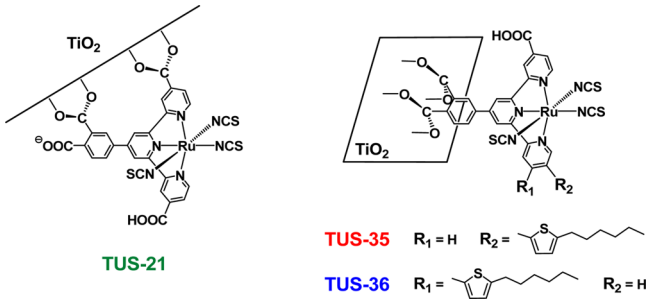

Figure 6. Speculated binding manners of **TUS-21**, **TUS-35**, and **TUS-36** at the TiO_2 surface.

In addition, some amount of **TUS-35** and **TUS-36** could not be desorbed from the TiO_2 photoelectrodes by immersing in a NaOH solution or a methanolic solution of TBAOH, even though **TUS-35** and **TUS-36** were dissolved well in these two solutions. These results suggest strongly that **TUS-35** and **TUS-36** adsorb dominantly to the TiO_2 photoelectrode using the 3,4-dicarboxyphenyl unit just like **TUS-20** (Figure 6), even though **TUS-35** and **TUS-36** have a COOH group at the terminal pyridine just like **TUS-21**. In these cases, a high conversion efficiency is not expected due to the unfavorable binding manners for the effective electron injection process in the DSCs as mentioned above.

It seems to be quite important to know the reason why the binding manners of **TUS-35** and **TUS-36** are different from that of **TUS-21** toward the molecular design of highly efficient ruthenium sensitizers. One of the possible interpretations is that the amount of TBA^+ contained in **TUS-35** and **TUS-36** is different from that contained in **TUS-21**. As described above, **TUS-35** and **TUS-36** contain 1.25 equiv of TBA^+, while **TUS-21** possesses 2.0 equiv of TBA^+. Therefore, the COOH group at the 4-position of the phenyl unit of **TUS-21** exists as COO^- in a dye-adsorption solvent because the H^+ of this COOH group is replaced perfectly by TBA^+. On the other hand, the H^+ of the COOH group at the 4-position of the phenyl unit of **TUS-35** (and **TUS-36**) is replaced partially by TBA^+. Therefore, the COOH group at the 4-position of the phenyl unit of **TUS-35** (and **TUS-36**) is considered to exist mainly as COOH in a dye-adsorption solvent. This difference might affect the adsorption manners of ruthenium sensitizers because the reaction rates of the bond formations between the COO^- group of the sensitizer and the OH group at the TiO_2 surface, and between the COOH group of the sensitizer and the OH group at the TiO_2 surface, are considered to be different. Therefore, the adsorption behavior of **TUS-35** and **TUS-36** were further investigated after adjusting the amount of TBA^+ contained in these **TUS** sensitizers to 2.0 equiv by using deoxycholic acid tetrabutylammonium salt ((TBA)-[DCA]).[48−51] However, the adsorption behavior of these two **TUS** sensitizers did not change at all against the expectation. In addition, the solar cell performance of the DSCs with these **TUS** sensitizers was not improved either by this treatment. Consequently, the other reason, such as a structural difference, seems to affect mainly the binding manners of **TUS-35** and **TUS-36** at the TiO_2 photoelectrode.

Solar Cell Performances of the Dye-Sensitized Solar Cells. Solar cell performances of the DSCs with **TUS-35** and **TUS-36**, together with those of the DSCs with **TUS-21** and Black dye, are summarized in Table 2. As mentioned above,

Table 2. Solar Cell Performances of the DSCs with TUS-21, TUS-35, TUS-36, and Black Dye[a]

sensitizer	J_{sc} [mA/cm^2]	V_{oc} [V]	*FF*	η [%]	amount of dye adsorption [×10^{-7} mol/cm^2]
TUS-35	15.4	0.60	0.69	6.4	2.7[b]
TUS-36	14.4	0.57	0.69	5.7	2.9[b]
TUS-20[c]	17.19	0.61	0.712	7.47	2.6[b]
TUS-21[c]	20.83	0.68	0.704	10.0	2.1
Black dye[c]	21.61	0.70	0.716	10.8	2.3

[a]The electrolyte is an acetonitrile solution containing I_2 (0.05 M), LiI (0.1 M), DMPImI (0.6 M), and TBP (0.3 M). Film thickness and active area of TiO_2 photoelectrodes were ca. 45 μm and 0.26 cm^2, respectively. Irradiation was performed using the solar simulator (AM 1.5, 100 mW/cm^2). [b]Some amounts of adsorbed **TUS-20**, **TUS-35**, and **TUS-36** could not be desorbed from the TiO_2 photoelectrode. [c]Data taken from ref 42.

high conversion efficiencies could not be obtained in the DSCs with **TUS-35** and **TUS-36**. The *Jsc* values obtained in the DSCs with these TUS sensitizers were much smaller than that obtained in the DSC with **TUS-21**, even though the amounts of dye adsorption of these TUS sensitizers were larger than that of **TUS-21**. As shown in Figure 7, IPCE values of the DSCs with

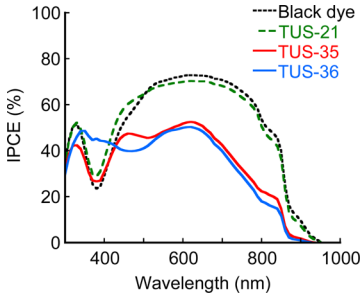

Figure 7. IPCE spectra of the DSCs with **TUS-21**, **TUS-35**, **TUS-36**, and Black dye.

TUS-35 and **TUS-36** at the wavelength range beyond 420 nm were much lower than those of the DSC with **TUS-21**. Since the energy levels of HOMO and LUMO, and the molar absorption coefficient at the whole visible region of **TUS-35** and **TUS-36**, were almost equal to those of **TUS-21**, the obtained smaller IPCE values of the **TUS-35** and **TUS-36** at the whole visible region seem to suggest that the effective electron injection does not occur due to the unfavorable binding manners at the TiO_2 surface. However, the main reason for the inferior performances of the DSCs with **TUS-35** and **TUS-36** is considered to be the promoted charge recombina-

DOI: 10.1021/am507442s
ACS Appl. Mater. Interfaces 2015, 7, 3152−3161

tion and/or charge transfer of the injected electrons in the TiO_2 photoelectrode to I_3^- in the electrolyte solution as discussed below.

On the other hand, the important aspect of the solar cell performances of two novel **TUS** sensitizers is that IPCE values at ~400 nm were improved largely only in the case of **TUS-36**, and these IPCE values were higher than those obtained in the DSCs with **TUS-21** and Black dye. The IPCE values of the DSCs at ~400 nm are generally lower due to the presence of I_3^- (or I_2) in the electrolyte solution with a high concentration. Therefore, this result indicates clearly that introduction of the hexylthiophene unit to the 4-position of the terpyridine-derived ligand is more effective than introducing this unit to the 5-position to overcome this drawback.

To obtain insight into the charge recombination and/or charge transfer of the injected electrons in the TiO_2 photoelectrode, open-circuit photovoltage decay (OCVD) measurements of the DSCs with **TUS** sensitizers were performed. The electron lifetimes in the TiO_2 photoelectrodes of the DSCs with **TUS-35** and **TUS-36** were found to be much shorter than those of the DSCs with **TUS-21** and Black dye at the matched V_{oc} values (Figure 8). These results suggest

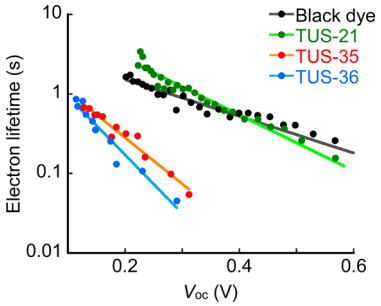

Figure 8. Electron lifetimes as a function of V_{oc} of the DSCs with **TUS-21**, **TUS-35**, **TUS-36**, and Black dye.

strongly that the charge recombination and/or charge transfer of the injected electrons in the TiO_2 photoelectrode is promoted quite largely in the DSCs with **TUS-35** and **TUS-36**. This promoted charge recombination and/or charge transfer in the DSCs with **TUS-35** and **TUS-36** seems to arise from the presence of the thiophene unit at the terpyridine-derived ligand. As reported previously, I_2 (or I_3^-) interacts with a thiophene and forms a charge transfer (CT) complex.[52−54] If **TUS-35** and **TUS-36** interact with I_2 (or I_3^-) through the S atom of thiophene unit, the local concentration of I_3^- is increased. In such cases, CT of the injected electrons in the TiO_2 photoelectrode to I_3^- would be promoted, which results in the shortening of the electron lifetime in the TiO_2 photoelectrode. In the cases of the DSCs with ruthenium sensitizers having an amine group at the ligand, CT of the injected electrons is reported to be enhanced due to the formation of a CT complex with I_2 (or I_3^-) through the N atom of amino group.[55−59] Therefore, it is likely that **TUS-35** and **TUS-36** interact with I_2 (or I_3^-) through the S atom of thiophene unit, which results in the promotion of CT of the injected electrons. On the other hand, the other possible interpretation is that the promoted CT of the injected electrons is attributed to the difference in the binding manners at the TiO_2 surface between **TUS** sensitizers (**TUS-35** and **TUS-36**) and **TUS-21**. It is reported that **TUS-20** adsorbs to the TiO_2 photoelectrode using the 3,4-dicarboxyphenyl unit just like **TUS-35** and **TUS-36**, and the electron lifetime in the TiO_2 photoelectrode of the DSC with **TUS-20** is extremely shorter than that of the DSC with **TUS-21**.[42] Therefore, these results suggest that the binding manner of ruthenium sensitizer is one of the important points to bring out fully the potential of photosensitizing ability of the ruthenium sensitizers.

Figure 9 shows Nyquist plots of the DSCs with **TUS-21**, **TUS-35**, **TUS-36**, and Black dye obtained from the electro-

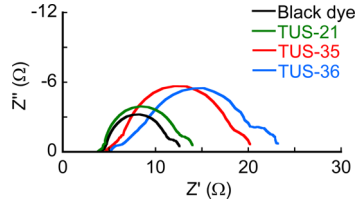

Figure 9. Nyquist plots of the DSCs with **TUS-21**, **TUS-35**, **TUS-36**, and Black dye under AM 1.5 irradiation conditions.

chemical impedance spectroscopic (EIS) measurements under AM 1.5 irradiation and open-circuit condition. The middle semicircle of Nyquist plot is assigned typically to the interfacial resistance at the TiO_2/dye/electrolyte interface (R2 resistance), which is related closely to the reaction rate of charge recombination and CT of the injected electrons. The large middle semicircle (R2 resistance) of the Nyquist plot under the irradiation condition suggests that charge recombination and/or CT of the injected electrons in the TiO_2 photoelectrode is promoted. As shown in Figure 9, R2 resistance of the DSCs with **TUS-35** and **TUS-36** was much larger than that of the DSC with **TUS-21**. These results indicate again that charge recombination and/or CT of the injected electrons is enhanced largely in the DSCs with **TUS-35** and **TUS-36**. We reported recently that the electron lifetime in the TiO_2 photoelectrode of the DSC with **TUS-20** is extremely shorter than that of the DSC with **TUS-21**.[42] The reason for this much shorter electron lifetime of **TUS-20** is considered to be attributed to the high I_3^- concentration at the TiO_2 surface. In the case of **TUS-20**, relatively large vacancy would exist at the **TUS-20**-adsorbed TiO_2 surface because **TUS-20** adsorbs to the TiO_2 photoelectrode using the 3,4-dicarboxyphenyl unit as shown in Figure 10.[42] In this case, I_3^- concentration at the TiO_2 surface would be higher, which induces the enhancement of the backward electron-transfer reaction to I_3^-. For comparison, such a vacancy is not considered to exist at the **TUS-21**-adsorbed TiO_2 surface because **TUS-21** adsorbs to the TiO_2 photoelectrode using one of the COOH groups at the terminal pyridines of the

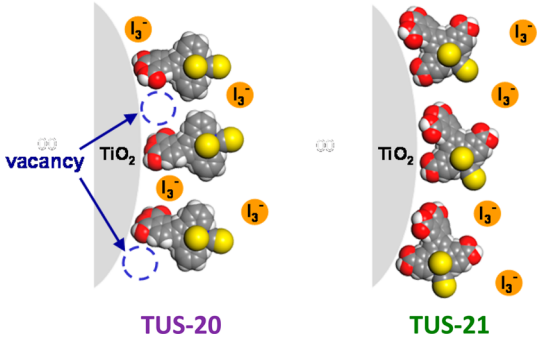

Figure 10. Speculated interfacial interaction between I_3^- and the TiO_2 surface (taken from ref 42).

DOI: 10.1021/am507442s
ACS Appl. Mater. Interfaces 2015, 7, 3152−3161

terpyridine-derived ligand and the COOH group at the 3-position of the phenyl unit.[42] In the cases of **TUS-35** and **TUS-36**, relatively large vacancy would exist because the adsorption manners of these two sensitizers are considered to be the same as that of **TUS-20**. Therefore, this binding manner seems to be a major reason for the promoted CT of the injected electrons in the TiO_2 photoelectrode to the I_3^- in the electrolyte solution in the cases of **TUS-35** and **TUS-36**.

CONCLUSIONS

Two novel ruthenium sensitizers with a hexylthiophene-modified terpyridine-derived ligand (**TUS-35** and **TUS-36**) have been synthesized to improve the molar absorption coefficient of **TUS-21**. A relatively strong absorption at ∼380 nm appeared, and the molar absorption coefficient at the MLCT band decreased in **TUS-35** by introducing a 2-hexylthiophene unit at the 5-position of the terpyridine-derived ligand. For comparison, a relatively strong absorption at ∼350 nm appeared without decreasing the molar absorption coefficient at the MLCT band in **TUS-36** by introducing a 2-hexylthiophene unit at the 4-position of the terpyridine-derived ligand. On the other hand, the energy levels of HOMOs and LUMOs of **TUS-35** and **TUS-36** were almost equal to those of **TUS-21**. Adsorption behavior of **TUS-35** and **TUS-36** to the TiO_2 surface was similar to that of **TUS-20** rather than that of **TUS-21**, suggesting that **TUS-35** and **TUS-36** adsorb to the TiO_2 photoelectrode using the 3,4-dicarboxyphenyl unit just like **TUS-20**.

The DSCs with **TUS-35** and **TUS-36** exhibited a relatively lower conversion efficiency (6.4% and 5.7%, respectively), while the DSC with **TUS-21** showed ∼10% efficiency under the AM 1.5 irradiation (100 mW/cm^2). Since the photo- and electrochemical properties of these two sensitizers are quite similar to those of **TUS-21**, unfavorable binding manners of **TUS-35** and **TUS-36** at the TiO_2 surface toward the electron injection process seem to be one reason for the inferior performance of these sensitizers. OCVD and EIS measurements of the DSCs with **TUS-35** and **TUS-36** revealed that charge recombination and/or CT of the injected electrons in the TiO_2 photoelectrode to I_3^- in the electrolyte solution is promoted largely compared to the DSC with **TUS-21**. Therefore, the inferior performances of **TUS-35** and **TUS-36** would be attributed mainly to this enhanced charge recombination and/or CT of the injected electrons. This study demonstrated that the position of the chromophore unit at the terpyridine-derived ligand affects only the photochemical properties of ruthenium sensitizers and also demonstrated that the binding manners of the ruthenium sensitizers at the TiO_2 photoelectrode affect largely the solar cell performances of the DSCs.

EXPERIMENTAL SECTION

Materials and General Measurements. Black dye,[7] 2-acetyl-4-bromopyridine,[43] 2-acetyl-5-bromopyridine,[44] and tributyl(5-hexylthiophene-2-yl)stannane[45,46] were prepared according to the previously reported methods. Characterization of the novel compounds prepared in this study was carried out by the previously reported procedures.[39−43,59] DFT MO calculations were performed by DMol^3 code package in Materials Studio 5.5 (Accelrys Inc.).[39−43,59]

Synthesis. *Compound 1*. 3,4-Dimethylbenzaldehyde (17.1 mmol, 2.3 g) and NaOH (27.5 mmol, 1.1 g) were dissolved in 80 mL of a mixed solution of ethanol and water (1:1, v/v). 2-Acetyl-4-methylpyridine (17.0 mmol, 2.3 g) was dissolved in 25 mL of ethanol, and this solution was added slowly to the former solution. This mixture was stirred for 12 h at room temperature. The yellow precipitate was filtered, washed with a mixed solvent of ethanol and water (1:4, v/v), and dried in vacuo; yield 4.1 g (96%). ^{1}H NMR (400 MHz, $CDCl_3$): δ = 8.66 (d, J = 4.8 Hz, 1H), 8.24 (d, J = 16.1 Hz, 1H), 8.02 (s, 1H), 7.90 (d, J = 15.8 Hz, 1H), 7.53 (s, 1H), 7.47 (d, J = 7.8 Hz, 1H), 7.35 (d, J = 4.0 Hz, 1H), 7.17 (d, J = 7.8 Hz, 1H), 2.50 (s, 3H), 2.30 (s, 3H), 2.29 (s, 3H).

Compound 4. 2-Acetyl-5-bromopyridine (compound **2**; 12.2 mmol, 2.45 g), compound **1** (12.2 mmol, 3.07 g), and KOH (35.3 mmol, 1.98 g) were dissolved in 120 mL of ethanol. NH_4OH solution (30%, 75 mL) was added to the solution, and then this mixture was stirred for 1 d at 60 °C. The pale yellow precipitate was filtered, washed with a mixed solvent of ethanol and water (1:2, v/v), and dried in vacuo; yield 2.3 g (44%). ^{1}H NMR (400 MHz, $CDCl_3$): δ = 8.79 (sd, J = 2.5 Hz, 1H), 8.77 (sd, J = 2.0 Hz, 1H), 8.72 (sd, J = 1.5 Hz, 1H), 8.68 (d, J = 5.0 Hz, 1H), 8.65 (d, J = 8.5 Hz, 1H), 8.57 (s, 1H), 8.03 (dd, J = 8.5 Hz, J' = 2.5 Hz, 1H), 7.73 (s, 1H), 7.68 (d, J = 7.5 Hz, 1H), 7.31−7.27 (m, 2H), 2.57 (s, 3H), 2.40 (s, 3H), 2.36 (s, 3H).

Compound 5. Compound **5** was synthesized according to the same procedure of compound **4**, except that 2-acetyl-4-bromopyridine was used instead of 2-acetyl-5-bromopyridine. Yield 73%. ^{1}H NMR (400 MHz, $CDCl_3$): δ = 8.85 (sd, J = 1.8 Hz, 2H), 8.74 (s, 1H), 8.67 (d, J = 4.8 Hz, 1H), 8.55 (d, J = 5.3 Hz, 1H), 8.50 (s, 1H), 7.75 (s, 1H), 7.70 (d, J = 8.3 Hz, 1H), 7.54 (dd, J = 5.3 Hz, J' = 2.0 Hz, 1H), 7.29−7.25 (m, 2H), 2.60 (s, 3H), 2.38 (s, 3H), 2.34 (s, 3H).

Compound 6. Compound **4** (3.6 mmol, 1.56 g) and $KMnO_4$ (34.8 mmol, 5.5 g) were suspended in 90 mL of a mixed solution of water and pyridine (1:2, v/v). This mixture was refluxed for 2 h. $KMnO_4$ (34.8 mmol, 5.5 g), water (10 mL), and pyridine (8 mL) were further added, and then this reaction mixture was refluxed for 2 h. This procedure was repeated four times to oxidize fully three methyl groups of compound **4**. MnO_2 was filtrated and then washed with water. The combined filtrates were condensed by evaporation, and then the pH value of the solution was adjusted to 1.0 by adding concentrated HCl. The pale yellow precipitate was filtrated, washed with water, and dried in vacuo; yield 1.7 g (90%). ^{1}H NMR (400 MHz, dimethyl sulfoxide (DMSO)): δ = 8.74−8.72 (m, 2H), 8.67 (d, J = 2.3 Hz, 1H), 8.55 (d, J = 1.5 Hz, 1H), 8.49 (d, J = 1.5 Hz, 1H), 8.29 (d, J = 8.5 Hz, 1H), 8.13 (dd, J = 8.5 Hz, J' = 2.4 Hz, 1H), 7.94−7.91 (m, 2H), 7.73 (dd, J = 4.8 Hz, J' = 1.6 Hz, 1H), 7.66 (d, J = 8.0 Hz, 1H).

Compound 7. Compound **7** was synthesized according to the same procedure of compound **6**, except that compound **5** was used instead of compound **4**. Yield 46%. ^{1}H NMR (400 MHz, DMSO): δ = 9.00−8.98 (m, 3H), 8.84 (sd, J = 1.8 Hz, 1H), 8.79 (sd, J = 1.8 Hz, 1H), 8.73 (sd, J = 1.8 Hz, 1H), 8.71 (d, J = 5.3 Hz, 1H), 8.16−8.14 (m, 2H), 7.97 (dd, J = 5.0 Hz, J' = 1.6 Hz, 1H), 7.87 (dd, J = 5.3 Hz, J' = 2.0 Hz, 1H).

Compound 8. Compound **6** (3.3 mmol, 1.7 g) was suspended in 500 mL of methanol. Concentrated H_2SO_4 (9 mL) was added, and then his mixture was refluxed for 12 h. 30% NH_4OH solution was added to adjust the pH value of this reaction mixture to 2.0. The white precipitate was filtrated, washed with water, and dried in vacuo; yield 0.63 g (34%). ^{1}H NMR (400 MHz, $CDCl_3$): δ = 9.13 (s, 1H), 8.89 (s, 1H), 8.78−8.75 (m, 3H), 8.62 (d, J = 7.5 Hz, 1H), 8.20 (s, 1H), 8.04 (d, J = 7.0 Hz, 2H), 7.93 (s, 2H), 4.05 (s, 3H), 3.97 (s, 3H), 3.96 (s, 3H).

Compound 9. Compound **9** was synthesized according to the same procedure of compound **8**, except that compound **7** was used instead of compound **6**. Yield 8%. ^{1}H NMR (400 MHz, $CDCl_3$): δ = 9.13 (s, 1H), 8.88 (d, J = 5.0 Hz, 1H), 8.86 (d, J = 1.5 Hz, 1H), 8.77 (d, J = 6.0 Hz, 2H), 8.55 (d, J = 5.0 Hz, 1H), 8.20 (d, J = 1.5 Hz, 1H), 8.05 (dd, J = 8.5 Hz, J' = 1.6 Hz, 1H), 7.94 (dd, J = 4.5 Hz, J' = 1.5 Hz, 1H), 7.91 (d, J = 8.0 Hz, 1H), 7.56 (dd, J = 5.0 Hz, J' = 2.0 Hz, 1H), 4.06 (s, 3H), 3.97 (s, 3H), 3.95 (s, 3H).

L-35′. Compound **8** (0.44 mmol, 0.25 g), tributyl(5-hexylthiophene-2-yl)stannane (0.52 mmol, 0.24 g), and $Pd(PPh_3)_4$ (0.013 mmol, 0.015 g) were dissolved in dry DMF (10 mL), and then this solution was stirred overnight at 85 °C under N_2 atmosphere. Most of the solvent was evaporated; the resulting residue was purified by a silica gel column chromatography using a mixed eluent of chloroform

DOI: 10.1021/am507442s
ACS Appl. Mater. Interfaces 2015, 7, 3152−3161

and methanol (100:1, v/v); yield 0.15 g (53%). ^{1}H NMR (400 MHz, $CDCl_3$): δ = 9.17 (s, 1H), 8.97 (sd, J = 2.0 Hz, 1H), 8.89 (d, J = 5.0 Hz, 1H), 8.85 (s, 1H), 8.77 (sd, J = 1.5 Hz, 1H), 8.73 (d, J = 8.0 Hz, 1H), 8.23 (sd, J = 1.5 Hz, 1H), 8.12−8.07 (m, 2H), 7.94−7.92 (m, 2H), 7.32−7.31 (m, 1H), 6.85 (d, J = 2.5 Hz, 1H), 4.06 (s, 3H), 3.98 (s, 3H), 3.96 (s, 3H), 2.88 (t, J = 7.5 Hz, 2H), 1.76−1.73 (m, 2H), 1.45−1.41 (m, 2H), 1.36−1.34 (m, 4H), 0.92 (t, J = 7.0 Hz, 3H).

L-36′. **L-36′** was synthesized according to the same procedure of **L-35′**, except that compound **9** was used instead of compound **8**. Yield 60%. ^{1}H NMR (400 MHz, $CDCl_3$): δ = 9.24 (s, 1H), 8.89 (d, J = 5.0 Hz, 1H), 8.87 (s, 1H), 8.77 (d, J = 6.0 Hz, 2H), 8.67 (d, J = 5.5 Hz, 1H), 8.22 (sd, J = 2.0 Hz, 1H), 8.07 (dd, J = 7.5 Hz, J' = 1.6 Hz, 1H), 7.94 (m, 2H), 7.54−7.51 (m, 2H), 6.88 (d, J = 3.5 Hz, 1H), 4.06 (s, 3H), 3.98 (s, 3H), 3.96 (s, 3H), 2.89 (t, J = 7.5 Hz, 2H), 1.78−1.74 (m, 2H), 1.45−1.41 (m, 2H), 1.37−1.33 (m, 4H), 0.94−0.91 (m, 3H).

L-35. **L-35′** (0.77 mmol, 0.5 g) was suspended in 50 mL of a mixed solution of acetone and 0.1 M NaOH solution (3:2, v/v), and then this mixture was refluxed for 5 h. After most of the acetone was removed by evaporation, concentrated HCl was added to adjust the pH value of this solution to 1.0. The pale yellow precipitate was filtrated, washed with water, and dried in vacuo; yield 0.4 g (85%). ^{1}H NMR (400 MHz, DMSO): δ = 9.05 (sd, J = 2.5 Hz, 1H), 9.04 (s, 1H), 8.98 (d, J = 5.0 Hz, 1H), 8.80 (s, 2H), 8.61 (d, J = 8.5 Hz, 1H), 8.29 (dd, J = 8.0 Hz, J' = 1.6 Hz, 2H), 8.17 (d, J = 8.0 Hz, 1H), 7.97 (d, J = 5.0 Hz, 2H), 7.57 (d, J = 3.5 Hz, 1H), 6.96 (d, J = 3.5 Hz, 1H), 2.86 (t, J = 7.5 Hz, 2H), 1.69−1.66 (m, 2H), 1.38−1.30 (m, 6H), 0.89−0.86 (m, 3H).

L-36. **L-36** was synthesized according to the same procedure of **L-35**, except that **L-36′** was used instead of **L-35′**. Yield 85%. ^{1}H NMR (400 MHz, DMSO): δ = 9.10 (s, 1H), 8.98 (d, J = 4.5 Hz, 1H), 8.78 (dd, J = 9.0 Hz, J' = 1.5 Hz, 2H), 8.74 (d, J = 5.0 Hz, 1H), 8.71 (s, 1H), 8.26 (s, 1H), 8.17 (dd, J = 8.0 Hz, J' = 2.0 Hz, 1H), 7.97 (d, J = 3.5 Hz, 2H), 7.77 (dd, J = 5.0 Hz, J' = 2.0 Hz, 1H), 7.72 (d, J = 3.5 Hz, 1H), 7.00 (d, J = 3.5 Hz, 1H), 2.88 (t, J = 7.5 Hz, 2H), 1.71−1.67 (m, 2H), 1.38−1.29 (m, 6H), 0.89−0.85 (m, 3H).

Ru(L-35)Cl$_3$ and Ru(L-36)Cl$_3$. $RuCl_3 \cdot 3H_2O$ (1.64 mmol, 0.43 g) and **L-35** (or **L-36**, 1.65 mmol, 1.0 g) were suspended in 150 mL of ethanol. This mixture was refluxed for 5 h under N_2 atmosphere. All the ethanol was removed by evaporation, and the dark brown residue was dried in vacuo; quantitative yield.

TUS-35. Ru(**L-35**)Cl_3 (1.64 mmol, 1.4 g) and KSCN (49.4 mmol, 4.8 g) were suspended in 125 mL of a mixed solution of H_2O and DMF (1:4, v/v). This mixture was refluxed for 1 d in the dark under N_2 atmosphere. 1400 mL of water was added to this reaction mixture, and then the pH value of this solution was adjusted to 1.0 by adding 0.5 M HCl. The precipitate was filtrated and dried in vacuo. This crude product was purified by a silica gel column chromatography using a mixed solvent of CH_3CN, saturated KNO_3 (aq), and H_2O (14:2:1, v/v). The second green band was collected, and then most of the CH_3CN was removed by evaporation. After 0.5 M HCl was added to the solution, the precipitate was filtrated. The obtained precipitate was once dissolved in the minimum amount of mixed solution of acetonitrile and 0.1 M TBAOH solution (10:3, v/v), and then it was further purified by the same procedure. Yield 15 mg (10%). ^{1}H NMR (400 MHz, CD_3CN): δ = 9.17 (d, J = 6.0 Hz, 1H), 9.12 (sd, J = 2.0 Hz, 1H), 8.82 (s, 1H), 8.60 (s, 1H), 8.57 (s, 1H), 8.42 (s, 1H), 8.31 (d, J = 8.5 Hz, 1H), 8.14−8.06 (m, 4H), 7.52 (d, J = 3.5 Hz, 1H), 6.94 (d, J = 3.5 Hz, 1H), 3.10−3.06 (m, 10H), 2.94 (t, J = 7.6 Hz, 2H), 1.80−1.76 (m, 2H), 1.65−1.57 (m, 10H), 1.40−1.31 (m, 16H), 0.99−0.95 (m, 18H). ESI-TOF MS (negative ion, CH_3CN): 823.82 m/z ([**M**-SCN-H]$^-$). Anal. Calcd for $C_{37}H_{29}N_6O_6S_4Ru \cdot 1.25(NC_{16}H_{36})$ ((TBA)[**M**]·0.25TBA): C, 57.72; H, 6.29; N, 8.56. Found: C, 57.99; H, 6.31; N, 8.29%.

TUS-36. **TUS-36** was synthesized according to the same procedure of **TUS-35**, except that Ru(**L-36**)Cl_3 was used instead of Ru(**L-35**)Cl_3. Yield 11%. ^{1}H NMR (400 MHz, CD_3CN): δ = 9.17 (d, J = 5.5 Hz, 1H), 8.85 (s, 1H), 8.76 (d, J = 6.0 Hz, 1H), 8.73 (s, 1H), 8.64 (s, 2H), 8.53 (s, 1H), 8.26−8.23 (m, 1H), 8.18 (dd, J = 8.0 Hz, J' = 2.2 Hz, 1H), 8.13 (dd, J = 6.0 Hz, J' = 1.6 Hz, 1H), 7.78 (d, J = 4.0 Hz, 1H), 7.75 (d, J = 5.5 Hz, 1H), 7.04 (d, J = 3.5 Hz, 1H), 3.12−3.07 (m, 10H), 2.98 (t, J = 7.7 Hz, 2H), 1.82−1.78 (m, 2H), 1.66−1.58 (m, 10H), 1.41−1.33 (m, 16H), 1.00−0.94 (m, 18H). ESI-TOF MS (negative ion, CH_3CN): 824.02 m/z ([**M**-SCN-H]$^-$). Anal. Calcd for $C_{37}H_{29}N_6O_6S_4Ru \cdot 1.25(NC_{16}H_{36})$ ((TBA)[**M**]·0.25TBA): C, 57.72; H, 6.29; N, 8.56. Found: C, 57.70; H, 6.63; N, 8.18%.

Preparation of TiO_2 Photoelectrodes and Dye-Sensitized Solar Cells. TiO_2 photoelectrodes were prepared by the previously reported procedures.[27−29] Film thickness and the active area of the TiO_2 photoelectrodes were ∼40 μm and 0.26 cm^2, respectively. **TUS-35** and **TUS-36** were dissolved in 1-propanol solution at the concentration of 0.2 mM, which contained 20 mM DCA.[60] The TiO_2 photoelectrode was immersed in each dye solution for 22 h at room temperature to adsorb the dye onto the TiO_2 surface. Photoelectrochemical measurements were carried out by the previously reported methods.[27−29] Electrolyte of the DSC was an acetonitrile solution containing I_2 (0.05 M), LiI (0.1 M), 1,3-dimethylimidazolium iodide (DMPImI) (0.6 M), and TBP (0.3 M). **TUS-35** and **TUS-36** were desorbed from the TiO_2 photoelectrode by immersing in a 0.05 M NaOH solution. The amount of dye adsorption was calculated from the absorption spectrum of the resulting solution, although some amounts of adsorbed **TUS-35** and **TUS-36** could not be desorbed from the TiO_2 photoelectrodes by this treatment.

AUTHOR INFORMATION

Corresponding Author

*E-mail: h.arakawa@ci.kagu.tus.ac.jp. Fax: (+81) 3 5261 4631. Phone: (+81) 3 5228 8311.

Notes

The authors declare no competing financial interest.

ACKNOWLEDGMENTS

This work was supported by the New Energy and Industrial Technology Development Organization (NEDO) of Japan. H.O. acknowledges a Grant-in-Aid for young scientist (B, No. 25810043) from the Ministry of Education, Culture, Sports, Science, and Technology of Japan.

REFERENCES

(1) O'Regan, B.; Grätzel, M. A Low-Cost, High-Efficiency Solar Cell Based on Dye-Sensitized Colloidal TiO_2 Films. *Nature* **1991**, *353*, 737−740.

(2) Nazeeruddin, M. K.; Kay, A.; Rodicio, I.; Humphry-Baker, R.; Müller, E.; Liska, P.; Vlachopoulos, N.; Grätzel, M. Conversion of Light to Electricity by *cis*-X_2-bis(2,2′-bipyridyl-4,4′-dicarboxylate)-ruthenium(II) Charge-Transfer Sensitizers (X = Cl$^-$, Br$^-$, I$^-$, CN$^-$, and SCN$^-$) on Nanocrystalline Titanium Dioxide Electrodes. *J. Am. Chem. Soc.* **1993**, *115*, 6382−6390.

(3) Grätzel, M. Recent Advances in Sensitized Mesoscopic Solar Cells. *Acc. Chem. Res.* **2009**, *42*, 1788−1798.

(4) Hagfeldt, A.; Boschloo, G.; Sun, L.; Kloo, L.; Pettersson, H. Dye-Sensitized Solar Cells. *Chem. Rev.* **2010**, *110*, 6595−6663.

(5) Yum, J.-H.; Baranoff, E.; Wenger, S.; Nazeeruddin, M. K.; Grätzel, M. Panchromatic Engineering for Dye-Sensitized Solar Cells. *Energy. Environ. Sci.* **2011**, *4*, 842−857.

(6) Nazeeruddin, M. K.; Zakeeruddin, S. M.; Humphry-Baker, R.; Jirousek, M.; Liska, P.; Vlachopoulos, N.; Shklover, V.; Fischer, C.-H.; Grätzel, M. Acid-Base Equilibria of (2,2′-Bipyridyl-4,4′-dicarboxylic acid)ruthenium(II) Complexes and the Effect of Protonation on Charge-Transfer Sensitization of Nanocrystalline Titania. *Inorg. Chem.* **1999**, *38*, 6298−6305.

(7) Nazeeruddin, M. K.; Péchy, P.; Renouard, T.; Zakeeruddin, S. M.; Humphyry-Baker, R.; Comte, P.; Liska, P.; Cevey, L.; Costa, E.; Shklover, V.; Spiccia, L.; Deacon, G. B.; Bignozzi, C. A. Engineering of Efficient Panchromatic Sensitizers for Nanocrystalline TiO_2-Based Solar Cells. *J. Am. Chem. Soc.* **2001**, *123*, 1613−1624.

(8) Nazeeruddin, M. K.; Angelis, F. D.; Fantacci, S.; Selloni, A.; Viscardi, G.; Liska, P.; Ito, S.; Takeru, B.; Grätzel, M. Combined Experimental and DFT-TDDFT Computational Study of Photo-

DOI: 10.1021/am507442s
ACS Appl. Mater. Interfaces 2015, 7, 3152−3161

electrochemical Cell Ruthenium Sensitizers. *J. Am. Chem. Soc.* **2005**, *127*, 16835−16847.
(9) Gao, F.; Wang, Y.; Shi, D.; Zhang, J.; Wang, M.; Jing, X.; Humphyry-Baker, R.; Wang, P.; Zakeeruddin, S. M.; Grätzel, M. Enhance the Optical Absorptivity of Nanocrystalline TiO_2 Film with High Molar Extinction Coefficient Ruthenium Sensitizers for High Performance Dye-Sensitized Solar Cells. *J. Am. Chem. Soc.* **2008**, *130*, 10720−10728.
(10) Chen, C.-Y.; Wang, M.; Li, J.-Y.; Pootrakulchote, N.; Alibabaei, L.; Ngocle, C.; Decoppet, J.-D.; Tsai, J.; Grätzel, C.; Wu, C.-G.; Zakeeruddin, S. M.; Grätzel, M. Highly Efficient Light-Harvesting Ruthenium Sensitizer for Thin-Film Dye-Sensitized Solar Cells. *ACS Nano* **2009**, *10*, 3103−3109.
(11) Cao, Y.; Bai, Y.; Yu, Q.; Cheng, Y.; Li, S.; Shi, D.; Gao, F.; Wang, P. Dye-Sensitized Solar Cells with a High Absorptivity Ruthenium Sensitizer Featuring a 2-(Hexylthio)thiophene Conjugated Bipyridine. *J. Phys. Chem. C* **2009**, *113*, 6290−6297.
(12) Vougioukalakis, G. C.; Philippopoulos, A. I.; Stergiopoulos, T.; Falaras, P. Contributions to the Development of Ruthenium-Based Sensitizers for Dye-Sensitized Solar Cells. *Coord. Chem. Rev.* **2011**, *255*, 2602−2621.
(13) Abbotto, A.; Manfredi, N. Electron-Rich Heteroaromatic Conjugated Polypyridine Ruthenium Sensitizers for Dye-Sensitized Solar Cells. *Dalton Trans.* **2011**, *40*, 12421−12438.
(14) Robson, K. C. D.; Bomben, P. G.; Berlinguette, C. P. Cycloruthenated Sensitizers: Improving the Dye-Sensitized Solar Cell with Classical Inorganic Chemistry Principles. *Dalton Trans.* **2012**, *41*, 7814−7829.
(15) Funaki, T.; Funakoshi, H.; Kitao, O.; Onozawa-Komatsuzaki, N.; Kasuga, K.; Sayama, K.; Sugihara, H. Cyclometalated Ruthenium-(II) Complexes as Near-IR Sensitizers for High Efficiency Dye-Sensitized Solar Cells. *Angew. Chem., Int. Ed.* **2012**, *51*, 7528−7531.
(16) Numata, Y.; Singh, S. P.; Islam, A.; Iwamura, M.; Imai, A.; Nozaki, K.; Han, L. Enhanced Light-Harvesting Capability of a Panchromatic Ru(II) Sensitizer Based on π-Extended Terpyridine with a 4-Methylstylryl Group for Dye-Sensitized Solar Cells. *Adv. Funct. Mater.* **2013**, *23*, 1817−1823.
(17) Imahori, H.; Umeyama, T.; Ito, S. Large π-Aromatic Molecules as Potential Sensitizers for Highly Efficient Dye-Sensitized Solar Cells. *Acc. Chem. Res.* **2009**, *42*, 1809−1818.
(18) Martínes-Díaz, M. V.; Torre, G.; Torres, T. Lighting Porphyrins and Phthalocyanines for Molecular Photovoltaics. *Chem. Commun.* **2010**, *46*, 7090−7108.
(19) Yella, A.; Lee, H.-W.; Tsao, H. N.; Yi, C.; Chandiran, A. K.; Nazeeruddin, M. K.; Diau, E. W.-G.; Yeh, C.-Y.; Zakeeruddin, S. M.; Grätzel, M. Porphyrin-Sensitized Solar Cells with Cobalt (II/III)-Based Redox Electrolyte Exceed 12% Efficiency. *Science* **2011**, *334*, 629−634.
(20) Mathew, S.; Yella, A.; Gao, P.; Humphry-Baker, R.; Curchod, B. F. E.; Ashari-Astani, N.; Tavernelli, I.; Rothlisberger, U.; Nazeeruddin, M. K.; Grätzel, M. Dye-Sensitized Solar Cells with 13% Efficiency Achieved Through the Molecular Engineering of Porphyrin Sensitizers. *Nat. Chem.* **2014**, *6*, 242−247.
(21) Yella, A.; Mai, C.-L.; Zakeeruddine, S. M.; Chang, S.-N.; Hsieh, C.-H.; Yeh, C.-Y.; Grätzel, M. Molecular Engineering of Push-Pull Porphyrin Dyes for Highly Efficient Dye-Sensitized Solar Cells: The Role of Benzene Spacers. *Angew. Chem., Int. Ed.* **2014**, *53*, 2973−2977.
(22) Chiba, Y.; Islam, A.; Watanabe, Y.; Komiya, R.; Koide, N.; Han, L. Dye-Sensitized Solar Cells with Conversion Efficiency of 11.1%. *Jpn. J. Appl. Phys.* **2006**, *45*, L638−L640.
(23) Ogura, R.; Nakane, S.; Morooka, M.; Orihashi, M.; Suzuki, Y.; Noda, K. High-Performance Dye-Sensitized Solar Cell with a Multiple Dye System. *Appl. Phys. Lett.* **2009**, *94*, 073308−1−3.
(24) Han, L.; Islam, A.; Chen, H.; Malapaka, C.; Chiranjeevi, B.; Zhang, S.; Yang, X.; Yanagida, M. High-Efficiency Dye-Sensitized Solar Cell with a Novel Co-adsorbent. *Energy Environ. Sci.* **2012**, *5*, 6057−6060.
(25) Numata, Y.; Zhang, S.; Yang, X.; Han, L. Cosensitization of Ruthenium-Polypyridyl Dyes with Organic Dyes in Dye-sensitized Solar Cells. *Chem. Lett.* **2013**, *42*, 1328−1335.
(26) Zhang, S.; Islam, A.; Yang, X.; Qin, C.; Zhang, K.; Numata, Y.; Chen, H.; Han, L. Improvement of Spectral Response by Co-sensitizers for High Efficiency Dye-Sensitized Solar Cells. *J. Mater. Chem. A* **2013**, *1*, 4812−4819.
(27) Ozawa, H.; Shimizu, R.; Arakawa, H. Significant Improvement in the Conversion Efficiency of Black-Dye-Based Dye-Sensitized Solar Cells by Cosensitization with Organic Dye. *RSC Adv.* **2012**, *2*, 3198−3200.
(28) Ozawa, H.; Okuyama, Y.; Arakawa, H. Effects of Cation Composition in the Electrolyte on the Efficiency Improvement of Black Dye-Based Dye-Sensitized Solar Cells. *RSC Adv.* **2013**, *3*, 9175−9177.
(29) Ozawa, H.; Okuyama, Y.; Arakawa, H. Dependence of the Efficiency Improvement of Black-Dye-Based Dye-Sensitized Solar Cells on Alkyl Chain Length of Quaternary Ammonium Cations in Electrolyte Solutions. *ChemPhysChem* **2014**, *15*, 1201−1206.
(30) Chen, B.-S.; Chen, K.; Hong, Y.-H.; Liu, W.-H.; Li, T.-H.; Lai, C.-H.; Chou, P.-T.; Chi, Y.; Lee, G.-H. Neutral, Panchromatic Ru(II) Terpyridine Sensitizers Bearing Pyridine Pyrazolate Chelates with Superior DSSC Performance. *Chem. Commun.* **2009**, 5844−5846.
(31) Chou, C.-C.; Wu, K.-L.; Chi, Y.; Hu, W.-P.; Yu, S. J.; Lee, G.-H.; Lin, C.-L.; Chou, P.-T. Ruthenium(II) Sensitizers with Heteroleptic Tridentate Chelates for Dye-Sensitized Solar Cells. *Angew. Chem., Int. Ed.* **2011**, *50*, 2054−2058.
(32) Wu, K.-L.; Li, C.-H.; Chi, Y.; Clifford, J. N.; Cabau, L.; Palomares, E.; Cheng, Y.-M.; Pan, H.-A.; Chou, P.-T. Dye Molecular Structure Device Open-Circuit Voltage Correlation in Ru(II) Sensitizers with Heteroleptic Tridentate Chelates for Dye-Sensitized Solar Cells. *J. Am. Chem. Soc.* **2012**, *134*, 7488−7496.
(33) Yang, S.-H.; Wu, K.-L.; Chi, Y.; Cheng, Y.-M.; Chou, P.-T. Tris(thiocyanate) Ruthenium(II) Sensitizers with Functionalized Dicarboxyterpyridine for Dye-Sensitized Solar Cells. *Angew. Chem., Int. Ed.* **2011**, *50*, 8270−8274.
(34) Lin, H.-W.; Wang, Y.-S.; Huang, Z.-Y.; Lin, Y.-M.; Chen, C.-W.; Yang, S.-H.; Wu, K.-L.; Chi, Y.; Liu, S.-H.; Chou, P.-T. Origins of Device Performance in Dicarboxyterpyridine Ru(II) Dye-Sensitized Solar Cells. *Phys. Chem. Chem. Phys.* **2012**, *14*, 14190−14195.
(35) El-Shafei, A.; Hussain, M.; Atiq, A.; Islam, A.; Han, L. A Novel Carbazole-Based Dye Outperformed the Benchmark Dye N719 for High Efficiency Dye-Sensitized Solar Cells. *J. Mater. Chem.* **2012**, *22*, 24048−24056.
(36) Hussain, M.; El-Shafei, A.; Islam, A.; Han, L. Structure-Property Relationship of Extended π-Conjugation of Ancillary Ligands with and without an Electron Donor of Heteroleptic Ru(II) Bipyridyl Complexes for High Efficiency Dye-Sensitized Solar Cells. *Phys. Chem. Chem. Phys.* **2013**, *15*, 8401−8408.
(37) El-Shafei, A.; Hussain, M.; Islam, A.; Han, L. Influence of Cyclic Versus Acyclic Oxygen-Containing Electron Donor Ancillary Ligands on the Photocurrent, Photovoltage and Photostability for High Efficiency Dye-Sensitized Solar Cells. *J. Mater. Chem. A* **2013**, *1*, 13679−13686.
(38) Kimura, M.; Masuo, J.; Tohata, Y.; Obuchi, K.; Masaki, N.; Murakami, T. N.; Koumura, N.; Hara, K.; Fukui, A.; Yamanaka, R.; Mori, S. Improvement of TiO_2/Dye/Electrolyte Interface Conditions by Positional Change of Alkyl Chains in Modified Panchromatic Ru Complex Dyes. *Chem.—Eur. J.* **2013**, *19*, 1028−1034.
(39) Ozawa, H.; Oura, S.; Shimizu, R.; Arakawa, H. Synthesis of a Novel Ruthenium Sensitizer Bearing an *ortho*-Dicarboxyphenyl Group as an Anchoring Unit for Dye-sensitized Solar Cells. *Chem. Lett.* **2012**, *41*, 1406−1408.
(40) Ozawa, H.; Yamamoto, Y.; Fukushima, K.; Yamashita, S.; Arakawa, H. Synthesis and Characterization of a Novel Ruthenium Sensitizer with a Hexylthiophene-functionalized Terpyridine Ligand for Dye-sensitized Solar Cells. *Chem. Lett.* **2013**, *42*, 897−899.
(41) Ozawa, H.; Fukushima, K.; Sugiura, T.; Urayama, A.; Arakawa, H. Ruthenium sensitizers having an *ortho*-dicarboxyl group as an

DOI: 10.1021/am507442s
ACS Appl. Mater. Interfaces 2015, 7, 3152−3161

anchoring unit for dye-sensitized solar cells: synthesis, photo- and electrochemical properties, and adsorption behavior to the TiO_2 surface. *Dalton Trans.* **2014**, *43*, 13208−13218.
(42) Ozawa, H.; Sugiura, T.; Shimizu, R.; Arakawa, H. Novel Ruthenium Sensitizers Having Different Numbers of Carboxyl Groups for Dye-Sensitized Solar Cells: Effects of the Adsorption Manner at the TiO_2 Surface on the Solar Cell Performance. *Inorg. Chem.* **2014**, *53*, 9375−9384.
(43) Ozawa, H.; Kuroda, T.; Harada, S.; Arakawa, H. Efficient Ruthenium Sensitizer with a Terpyridine Ligand Having a Hexylthiophene at the 4-position for Dye-Sensitized Solar Cells: Effects of the Substituent Position on the Solar Cell Performance. *Eur. J. Inorg. Chem.* **2014**, 4734−4739.
(44) Abarca, B.; Ballesteros, R.; Ballesteros-Garrido, R.; Colobert, F.; Leroux, F. R. Triazolopyridines. Part 26: The Preparation of Novel [1,2,3]triazolo[1,5-a]pyridine Sulfoxides. *Tetrahedron* **2008**, *64*, 3794−3801.
(45) Brusso, J. L.; Hirst, O. D.; Dadvand, A.; Ganesan, S.; Cicoira, F.; Robertson, C. M.; Oakley, R. T.; Rosei, F.; Perepichka, D. F. Two-Dimensional Structural Motif in Thienoacene Semiconductors: Synthesis, Structure, and Properties of Tetrathienoanthracene Isomers. *Chem. Mater.* **2008**, *20*, 2484−2494.
(46) Tian, N.; Thiessen, A.; Schiewek, R.; Schmitz, O. J.; Hertel, D.; Meerholz, K.; Holder, E. Efficient Synthesis of Carbazolyl- and Thienyl-Substituted β-Diketonates and Properties of Their Red- and Green-Light-Emitting Ir(III) Complexes. *J. Org. Chem.* **2009**, *74*, 2718−2725.
(47) García-Iglesias, M.; Yum, J.-H.; Humphry-Baker, R.; Zakeeruddin, S. M.; Péchy, P.; Vázquez, P.; Palomares, E.; Grätzel, M.; Nazeeruddin, M. K.; Torres, T. Effect of Anchoring Groups in Zinc Phthalocyanine on the Dye-Sensitized Solar Cell Performance and Stability. *Chem. Sci.* **2011**, *2*, 1145−1150.
(48) Neale, N. R.; Kopidakis, N.; Lagemaat, J.; Grätzel, M.; Frank, A. J. Effect of a Coadsorbent on the Performance of Dye-Sensitized TiO_2 Solar Cells: Shielding versus Band-Edge Movement. *J. Phys. Chem. B* **2005**, *109*, 23183−23189.
(49) Wu, K.-L.; Ho, S.-T.; Chou, C.-C.; Chang, Y.-C.; Pan, H.-A.; Chi, Y.; Chou, P.-T. Engineering of Osmium(II)-Based Light Absorbers for Dye-Sensitized Solar Cells. *Angew. Chem., Int. Ed.* **2012**, *51*, 5642−5646.
(50) Wu, K.-L.; Ku, W.-P.; Clifford, J. N.; Palomares, E.; Ho, S.-T.; Chi, Y.; Liu, S.-H.; Chou, P.-T.; Nazeeruddin, M. K.; Grätzel, M. Harnessing the Open-Circuit Voltage via a New Series of Ru(II) Sensitizers Bearing (*iso*-)uinolinyl Pyrazolate Ancillaries. *Energy Environ. Sci.* **2013**, *6*, 859−870.
(51) Chou, C.-C.; Chen, P.-H.; Hu, F.-C.; Chi, Y.; Ho, S.-T.; Kai, J.-J.; Liu, S.-H.; Chou, P.-T. Structural Tuning of Ancillary Chelate in Tri-Carboxyterpyridine Ru(II) Sensitizers for Dye Sensitized Solar Cells. *J. Mater. Chem. A* **2014**, *2*, 5418−5426.
(52) Lang, R. P. Molecular Complexes and Their Spectra. XV. Iodine Complexes with Thiophene, 2-Methylfuran and N-Methylpyrrole. *J. Am. Chem. Soc.* **1962**, *84*, 4438−4441.
(53) Näther, C.; Bolte, M. Investigations on the Interaction Between sp 2-Sulfur Atoms and Iodine Molecules Using the Cambridge Structural Database. *Phosphorus, Sulfur Silicon Relat. Elem.* **2003**, *178*, 453−464.
(54) Balanay, M. P.; Kim, D. H. Theoretical Study on the Correlations Between dye-Iodine Interactions and Open-Circuit Voltages in Dyes Containing Furan and Thiophene. *Comput. Theor. Chem.* **2014**, *1029*, 1−12.
(55) Huang, W.-K.; Cheng, C.-W.; Chang, S.-M.; Lee, Y.-P.; Diau, E. W.-G. Synthesis and Electron-Transfer Properties of Benzimidazole-Functionalized Ruthenium Complexes for Highly Efficient Dye-Sensitized Solar Cells. *Chem. Commun.* **2010**, *46*, 8992−8994.
(56) Reynal, A.; Forneli, A.; Martinez-Ferrero, E.; Sanchez-Diaz, A.; Vidal-Ferran, A.; O'Regan, B. C.; Palomares, E. Interfacial Charge Recombination Between e^--TiO_2 and the I^-/I_3^- Electrolyte in Ruthenium Heteroleptic Complexes: Dye Molecular Structure-Open Circuit Voltage Relationship. *J. Am. Chem. Soc.* **2008**, *130*, 13558−13567.
(57) Han, W.-S.; Han, J.-K.; Kim, H.-Y.; Choi, M. J.; Kang, Y.-S.; Pac, C.; Kang, S. O. Electronic Optimization of Heteroleptic Ru(II) Bipyridine Complexes by Remote Substituents: Synthesis, Characterization, and Application to Dye-Sensitized Solar Cells. *Inorg. Chem.* **2011**, *50*, 3271−3280.
(58) Li, X.; Reynal, A.; Barnes, P.; Humphry-Baker, R.; Zakeeruddin, S. M.; Angelis, F. D.; O'Regan, B. C. Measured Binding Coefficients for Iodine and Ruthenium Dyes; Implications for Recombination in Dye-Sensitized Solar Cells. *Phys. Chem. Chem. Phys.* **2012**, *14*, 15421−15428.
(59) Ozawa, H.; Kawaguchi, H.; Okuyama, Y.; Arakawa, H. Ruthenium Sensitizers with 2,2′-Bipyrimidine or a 5,5′-Disubstituted 2,2′-Bipyrimidine Ligand: Synthesis, Photo- and Electrochemical Properties, and Application to Dye-Sensitized Solar Cells. *Eur. J. Inorg. Chem.* **2013**, 5187−5195.
(60) Ozawa, H.; Awa, M.; Ono, T.; Arakawa, H. Effects of Dye-Adsorption Solvent on the Performances of the Dye-Sensitized Solar Cells Based on Black Dye. *Chem.—Asian J.* **2012**, *7*, 156−162.

DOI: 10.1021/am507442s
ACS Appl. Mater. Interfaces 2015, 7, 3152−3161